RSC Advances

PAPER

View Article Online
View Journal | View Issue

Cite this: *RSC Adv.*, 2025, **15**, 9854

Improved thermoelectric properties of α-phase Cu_2Se thin films through multiphase nanostructuring

Muhammad Faizan Masoud,[a] Sajid Butt,*[a] Muhammad Waseem Akram,[a] Nimra Naeem,[a] Awais Irfan,[a] Aumber Abbas[b] and Syed Irfan[c]

Received 15th January 2025
Accepted 22nd March 2025

DOI: 10.1039/d5ra00370a

rsc.li/rsc-advances

Copper selenide (Cu_2Se) has been extensively studied due to its promising thermoelectric properties in bulk form. However, the miniaturization of thermoelectric devices using thin films is highly desired for smart applications. To date, there are few reports on composite thin films of Cu_2Se for thermoelectric applications, primarily due to their lower conversion efficiency. In the present work, Cu_2Se-based multiphase nanocomposites are presented to demonstrate enhanced conversion efficiency. The detailed structural characterization reveals that thermally evaporated Te-doped Cu_2Se thin films have multiphase compositions. The electrical conductivity decreases after Te-doping, due to enormous scattering of carriers against secondary phases and lattice defects. However, upon further increasing Te-doping concentration, both the electrical conductivity and Seebeck coefficient start increasing simultaneously, due to the formation of Cu_2Te nanoclusters and Te–Se solid solution, in the matrix of Cu_2Se. We emphasize the power factor, with the highest value reaching 234.0 μW mK^{-2} at 400 K, as a key indicator of thermoelectric performance. A slightly overestimated value of dimensionless figure-of-merit (*ZT*) of 0.2 was obtained using the power factor and merely the electronic part of the thermal conductivity. The current synthesis route synergizes the effects of a multiphase system in thin film research to enhance the thermoelectric efficiency of Cu_2Se and related materials classes.

Introduction

The increasing demand for green energy arises from critical concerns about global warming and the heavy dependence on fossil fuels. A significant challenge that remains is improving the efficiency of energy conversion, as a large portion of energy is dissipated as waste heat. Thermoelectric devices have gained considerable attention for their ability in converting heat directly into electrical energy and *vice versa*. These thermoelectric devices are comprised of p-type and n-type material legs connected electrically in series and thermally parallel.[1] The conversion efficiency of a single leg material can be evaluated using a dimensionless figure-of-merit: $ZT = \left(\frac{\sigma S^2}{K}\right)T$; where, σS^2 is explicitly defined as power factor (PF), S, σ, k, and T are the Seebeck coefficient (thermopower), the electrical conductivity, the thermal conductivity, and the working temperature, respectively. The simultaneous suppression of thermal conductivity and enhancement of PF yields significant improvement in the performance of thermoelectric materials. Nonetheless, the intrinsic limitation of low conversion efficiency continues to impede their integration into practical thermoelectric (TE) applications.

Over the past decades, researchers have continued to explore a wide range of materials to enhance thermoelectric performance, from common metals to complex semiconductors.[2–5] Several classes of materials are being investigated in search of promising thermoelectric properties including but not limited to oxides,[4,6–12] skutterudites,[13,14] and chalcogenides.[15–25] They aim to enhance their thermoelectric properties through various strategies such as doping,[26–29] nano structuring,[14,20,23,30–34] and material hybridization.[35] Despite considerable progress, developing efficient, cost-effective, and environmentally friendly thermoelectric materials, remains a persistent challenge. Zhao *et al.*[36] recently reported an impressive *ZT* value of 2.6 in single-crystalline SnSe at 923 K due to the combined effects of ultralow thermal conductivity and high PF.

Among chalcogenides, Cu_2Se has received immense importance due to its phonon-liquid electron-crystal (PLEC) behavior.[19,35,37] The superionic $Cu_{2-x}Se$ attracts the attention of thermoelectric researchers due to its distinct thermal transport properties, which are linked to a structural shift that takes place at around 400 K.[38] Around 400 K, the $Cu_{2-x}Se$ solid state

[a]*Department of Space Science, Institute of Space Technology, Islamabad 44000, Pakistan. E-mail: sajid.butt@ist.edu.pk*

[b]*School of Materials Engineering, Jiangsu University of Technology, Changzhou 213001, China*

[c]*State Key Laboratory of Environment-Friendly Energy Materials, Southwest University of Science and Technology, Mianyang 621010, China*

undergoes a phase change from the low-temperature α-phase to the high-temperature β-phase.[39,40] In the compound, $Cu_{2-x}Se$, selenium (Se) atoms are situated within face-centered cubic (FCC) lattice sites in both of its phases.[41] However, the behavior of copper (Cu) atoms differs between the α-phase and the β-phase.[42,43] In the α-phase, Cu atoms demonstrate ordered and localized characteristics, while in the β-phase, they manifest disorder and superionic attributes. This superionic behavior arises from the movement of Cu ions under an applied electric field, leading to a decrease in their electrochemical potential.[40,44,45] The critical scattering of both phonons and charge carriers around 400 K greatly increases the *ZT* value, corresponding with the phonon-liquid electron-crystal (PLEG) concept.[17] Only in the critical scattering region, application into practical devices is hindered due to a lack of stability in the performance. Furthermore, thermoelectric performance significantly drops at higher temperatures, even if Cu_2Se achieves an ultrahigh $ZT > 2$ at 410 K.[46] Cu_2Se emerges as a highly intriguing thermoelectric material that produces surprisingly high *ZT* values range of 1.5–2.1 at temperatures close to 1000 K. The process of chemical synthesis can provide nanoparticles with precise sizes and shapes, potentially leading to a tighter grain boundary. Cu_2Se thermoelectric materials exhibit a *ZT* value exceeding 2 at high temperatures (800–1000 K), which is attributed to the "liquid-like" behavior of the β-phase with an anti-fluorite structure, as shown by both theoretical and experimental studies. Additionally, bulk Cu_2Se with a monoclinic α-phase demonstrates favorable thermoelectric performance near room temperature.[47] Day *et al.*, offer a theoretical prediction for the maximum *ZT* value of α-Cu_2Se, estimated to be around 1.16 at 305 K, which is comparable to that of standard thermoelectric materials.[48] Cu_2Se nanoparticles are synthesized by electrochemical procedure and their optical and electrical characterization are reported by Rong.[49] $Cu_{2-x}Se$-based chalcogenides attract significant attention as promising P-type thermoelectric materials, exhibiting a figure of merit (*ZT*) greater than unity.[40,44,50–52]

Copper chalcogenide thin films garner significant interest among researchers due to their wide range of applications in different optoelectronic devices.[53] Thermoelectric materials have a wide range of advanced applications beyond conventional power generation and cooling. They can harvest body heat to power wearable electronics, enabling continuous health monitoring or AI-driven hand motion recognition systems, as demonstrated in recent studies.[54] In robotics, thermoelectric generators (TEGs) capture waste heat from mechanical components, providing supplementary power for sensors and processors, enhancing energy efficiency and responsiveness in AI-integrated robotic hands.[55] Moreover, thermoelectric devices play a crucial role in fire alarming systems by detecting sudden temperature changes and generating small voltages to trigger alarms, offering a reliable, battery-free solution for fire detection.[56] In the field of smart buildings, integrating thermoelectric materials into building structures allows energy harvesting from temperature gradients, such as between indoor and outdoor surfaces, to power sensors and control systems, contributing to energy-efficient and sustainable infrastructure.[57] However, only a few reports can be found over thin films of Cu_2Se for thermoelectric applications.[58–61] Lin *et al.* synthesize Cu_2Se thin films using a solution-based method. This technique yields a maximum power factor (PF) of 6.2 $\mu W\,cm^{-1}\,K^{-2}$ on a rigid Al_2O_3 substrate and 4.6 $\mu W\,cm^{-1}\,K^{-2}$ on a flexible polyimide substrate.[62] They optimize the carrier concentration of Cu_2Se thin films using a soaking procedure in Cu^+ ion solution which further enhances the thermoelectric properties.[62,63] However, the Cu_2Se thin films demonstrated to date typically exhibit suboptimal thermoelectric performance, primarily attributable to structural imperfections such as voids and compositional defects within the films. High-temperature post-treatment is commonly used to improve and stabilize the thermoelectric (TE) performance of thin films. However, this method often weakens the bonding strength between the thin film and the substrate, especially when using organic flexible substrates. As a result, designing and fabricating Cu_2Se thin films with enhanced TE performance without relying on high-temperature processing remains a significant challenge.[64]

In this work, the thermoelectric transport properties of Te-doped Cu_2Se thin films have been systematically explored and explained with the aid of detailed structural characterizations. In our previous study, we employed X-ray absorption spectroscopy, an element-sensitive, orbital-specific, and local structural technique, to examine the atomic-scale structural influence of Te in the matrix of bulk Cu_2Se.[21] The results demonstrated the formation of Cu_2Te nanoclusters instead of Te replacing Se sites, indicating an essential approach to improve thermoelectric performance in Cu_2Se superionic conductors. Building on this idea, thin films through thermal evaporation have been fabricated and tested to strengthen the idea of miniaturization of thermoelectric devices.

Experimentation

The complete synthesis and characterization route has been demonstrated in Fig. 1. At first, pure and Te-doped Cu_2Se powdered samples were synthesized by ball milling followed by their compaction into pellets using spark plasma sintering (SPS), as the complete synthesis is given in ref. 21. A series of pure Cu_2Se and Te-doped $Cu_2Se_{0.95}Te_{0.05}$ (Te-5%), $Cu_2Se_{0.9}Te_{0.1}$ (Te-10%), and $Cu_2Se_{0.8}Te_{0.2}$ (Te-20%) films having a thickness of 100 nm were evaporated over glass substrates, under a vacuum environment maintained at 2.0×10^{-5} mbar through thermal evaporation technique (NANOVAK 3000TH). The bulk chunks of the materials to be evaporated were placed into a tungsten crucible and precleared glass slides were used as the substrates. The evaporation rate was fixed at 0.5 Å s^{-1} under the current ranging from 90 to 100 A. The samples were prepared and handled under vacuum (10^{-3} torr) to prevent oxidation and contaminations. The obtained thin films were annealed at 400 C under an inert environment.

The Cu and Se binding energies were determined by X-ray photoelectron spectroscopy (XPS) using a Thermo Scientific Escalab-250xi equipped with monochromatic Al Kα radiation. The effect of charging was corrected from the as-acquired data with respect to the C 1s peak (284.8 eV). XPSPEAK41 software

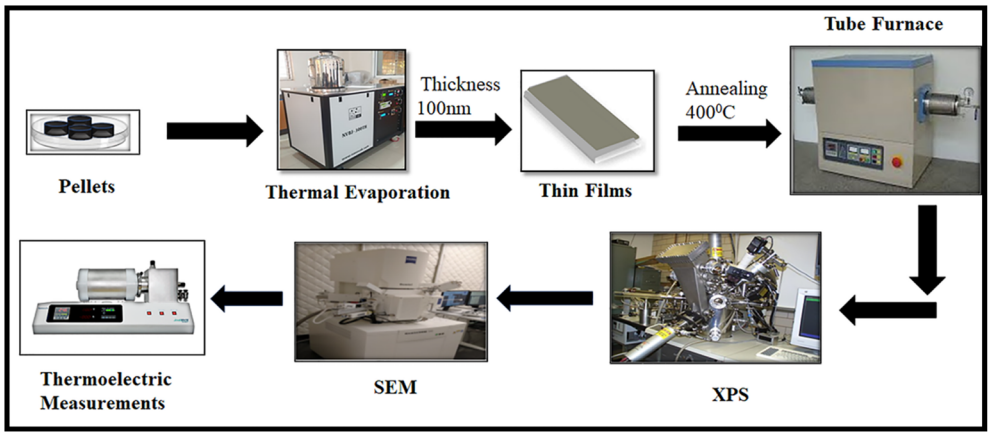

Fig. 1 Schematic of thermoelectric thin film fabrication and characterization process. Pellets are deposited *via* thermal evaporation to form 100 nm thin films, followed by annealing at 400 °C in a tube furnace. The films undergo structural and compositional analysis through XPS and SEM, with thermoelectric performance evaluated by a dedicated measurement system.

was used to deconvolute the high-resolution Cu 2p, Se 3d, and Te 3d spectra. The surface morphology and elemental composition of all series of thin films were determined using a scanning electron microscope (ZEISS Gemini SEM 300-8202017309) equipped with an energy-dispersive spectroscopy (EDS) detector. The electrical conductivity and Seebeck coefficient were measured simultaneously using a Thermoelectric Parameter Test System (Joule Yacht-NAMICRO-3L).

Results and discussion

The full survey scan for the pure $Cu_{2-x}Se$ and Te-doped (Te-20%) is shown in Fig. 2(a). The presence of Cu, Se and Te is evident from different core shell contributions. A strong peak around ~285 eV is assigned to C 1s employed for referencing to correct peak shift about surface charging as shown in Fig. 2(a). The high-resolution spectra of Cu 2p as taken from pure $Cu_{2-x}Se$ and Te-20% has been deconvoluted and shown in Fig. 2(b) and (c), respectively. The detailed analysis of Cu 2p data suggests the formation of $Cu_{2-x}Se$ as indicated by the presence of Cu^{1+} and Cu^{2+}. The presence of Cu^{2+} ions in $Cu_{2-x}Se$ is attributed to Cu vacancies caused by the ionic mobility of Cu and it also supports the superionic behavior $Cu_{2-x}Se$, as reported earlier.[19] Additionally, traces of CuO could also be detected due to surface oxidation of the films. After Te-doping, the formation of Cu_2Te was predominately detected as indicated by a synthetic peak at a lower energy, as shown in Fig. 2(c). These results are also supported by the high-resolution spectra of Se 3d as taken from pure $Cu_{2-x}Se$ as shown in Fig. 2(d), and high-resolution spectra of Se 3d and Te 3d ask taken from Te-20% as shown in Fig. 2(e) and (f), respectively. It is suggested that Te is present in multiphase system comprised of Te, Se–Te and Cu_2Te. Butt *et al.* has also reported that Te-doping results in the formation of Cu_2Te nanoclusters in the matrix of $Cu_{2-x}Se$ through the aid of X-ray absorption spectroscopy coupled with computational study.[21] Further, Te-doping has greatly suppressed the concentration of Cu^{2+} which infers reduced mobility of Cu ions in the lattice, which results in an improved thermal stability of $Cu_{2-x}Se$. This analysis demonstrates that Te-doping alters the electronic environment and bonding, which is essential for enhancing thermal stability and thermoelectric properties of $Cu_{2-x}Se$.

The surface morphology and phase distribution of pure $Cu_{2-x}Se$ film are shown in Fig. 3. The annealed films have shown a homogeneous and uniformly distributed grain structure with densely packed and well-connected grains as revealed by the secondary electron (SE) image, as shown in Fig. 3(a). Further, the image taken using in-lens detector has ruled out the presentence of any detectable secondary phase, as shown in Fig. 3(b). This homogeneity may provide better crystallinity leading towards better transport properties.[65] The average particle size was calculated approximately 140 nm, as shown in Fig. 3(c). The uniform distribution of $Cu_{2-x}Se$ grains can also be confirmed by EDS mapping, as shown in Fig. 3(d)–(f). The EDS of pure $Cu_{2-x}Se$ shows both Cu and Se are evenly distributed which indicates the uniformity of single phase $Cu_{2-x}Se$. The elemental analysis of pure and Te-20% thin film samples are given in Table 1. After Te-doping, significant changes in surface morphology have been observed as indicated by SEM analysis of Te-20%. Some smaller sized clusters of Cu_2Te can be seen as shown in Fig. 4(a), which could further be confirmed by in-lens image as shown in Fig. 4(b). The average particle size has been reduced due to the formation of nanoclusters of Cu_2Te in the matrix of $Cu_{2-x}Se$. The formation of Cu_2Te nanoclusters could further be confirmed from EDS mapping, as shown in Fig. 4(d)–(g). The EDS micrographs of the Te-20% thin film reveals even more pronounced changes in surface morphology. The grains appear irregular and uneven, with substantial agglomeration observed in Fig. 4(d)–(g). The surface becomes rougher and less homogeneous, likely due to the formation of Cu_2Te nanoclusters. The chemical state analysis has also suggests the formation of Cu_2Te phase which has been confirmed by SEM coupled with EDS analysis. The formation of secondary phases offer enormous scattering sites for charge carriers and phonons which may serve the purpose of energy filters.[22]

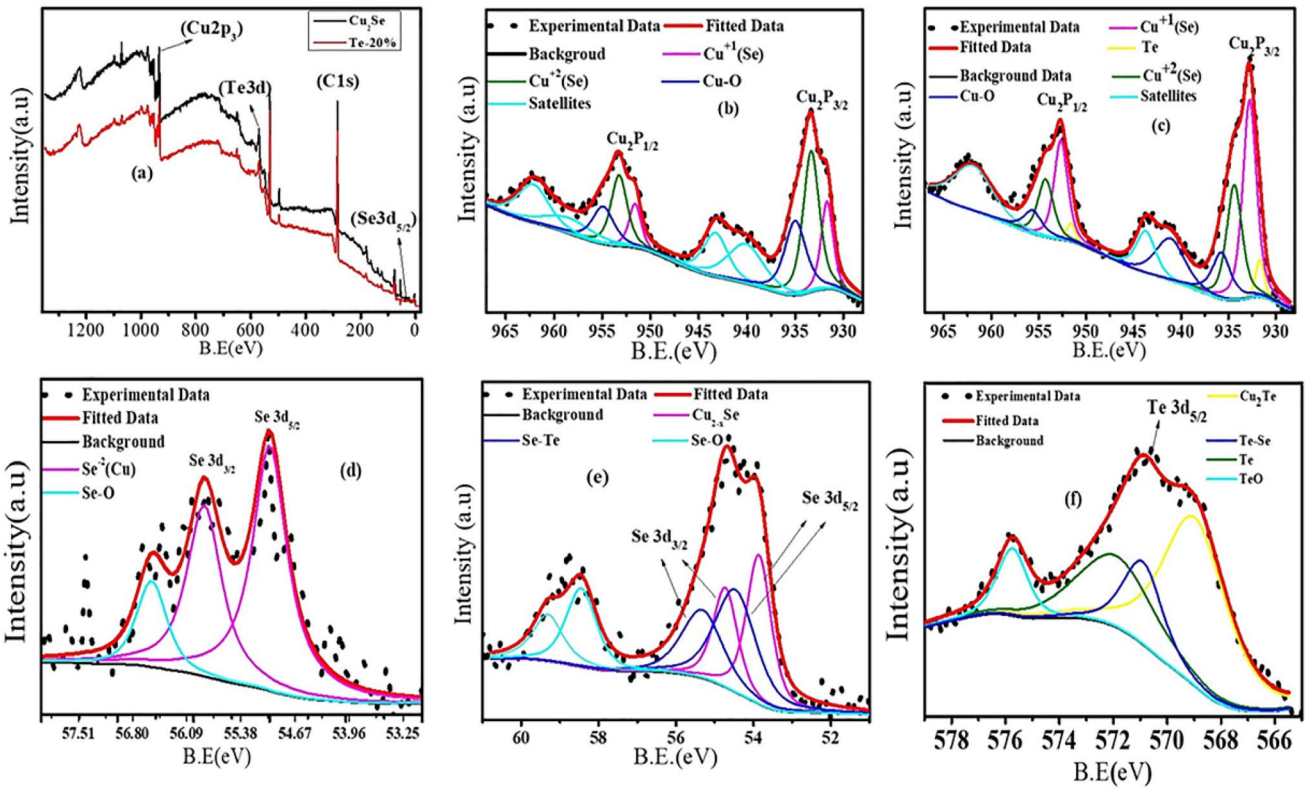

Fig. 2 The full survey XPS spectra for thin film specimens of Cu_2Se and $Cu_2Se_{0.8}Te_{0.2}$ (Te-20%) (a), the high-resolution spectra of Cu 2p from Cu_2Se (b), Te-20% (c), the high-resolution Se 3d spectra from Cu_2Se (d), Te-20% (e), and the high-resolution Te 3d spectra Te-20% (f).

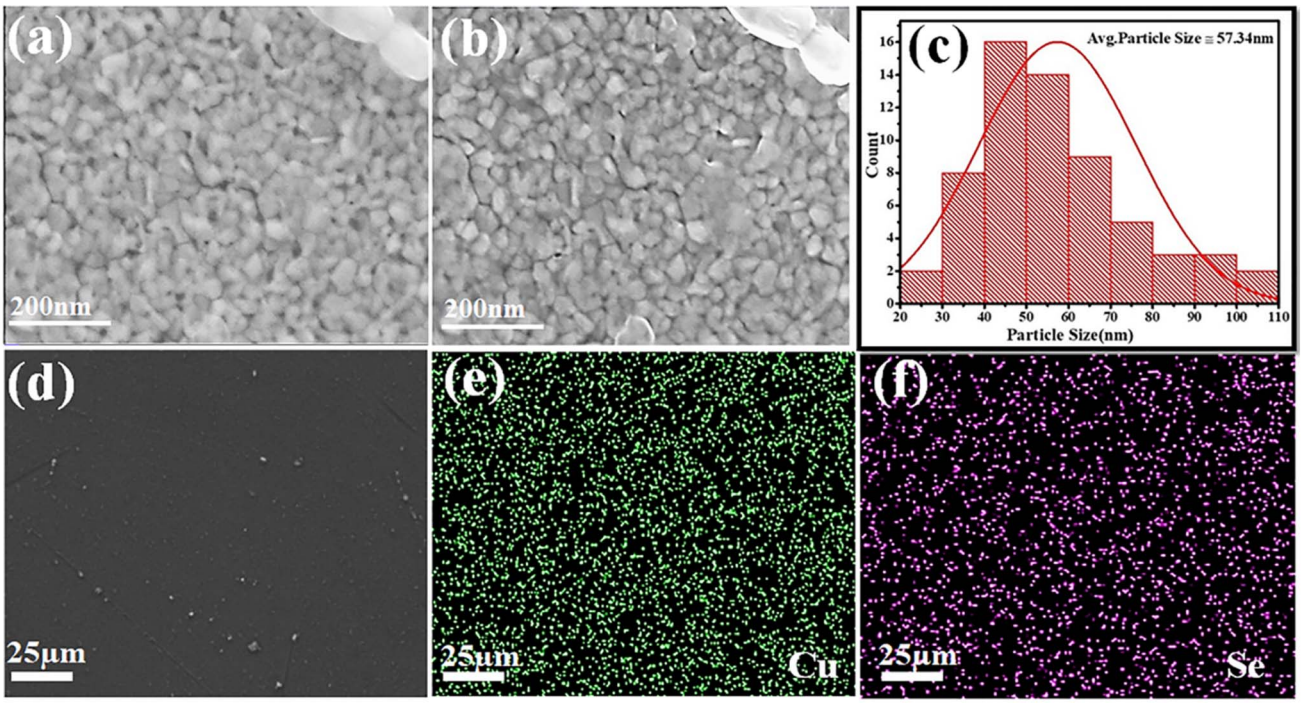

Fig. 3 Scanning electron microscopic (SEM) images of pure Cu_2Se thin film using (a) secondary electrons, (b) in-lens detector, (c) particle size, (d) SEM image used for elemental mapping of (e) Cu, (f) Se.

Table 1 Atomic percentages of Cu, Se, and, Te in pure and Te-doped (20%) samples, showing elemental composition changes after tellurium doping

Sample	Elements	Atomic (%)
Pure	Cu	62.8
	Se	37.2
Te-20%	Cu	74.5
	Se	23.2
	Te	2.3

The temperature dependence of TE properties of all the series of pure and Te-doped $Cu_{2-x}Se$ thin films has been measured in α-phase (below 410 K). The electrical conductivity (σ) of the pure $Cu_{2-x}Se$ is found to be the highest among all the compositions. However, after Te-doping, the electrical conductivity decreases as compared to the pure $Cu_{2-x}Se$, due increased carrier scattering against the defects introduced by Te-doping. Upon further increasing the Te content, the electrical conductivity begins increasing again. This increase is associated with the formation of Cu_2Te nanoclusters, as confirmed by the by XPS results as well. The higher intrinsic electrical conductivity of Cu_2Te phase offers electrical pathways in the matrix of $Cu_{2-x}Se$, which is also in good agreement with that of the previous reports.[21] The electrical conductivity of Te-20% has been observed to be highest among all the series of Te-doped samples.

Further, in order to inquire conduction mechanism, activation energy (E_g) was determined using Arrhenius equation, as given in eqn (1).

$$\sigma = \sigma_0 \exp\left(-\frac{E_g}{K_B T}\right) \quad (1)$$

where, σ, K_B, T and E_g are the electrical conductivity, Boltzmann constant and absolute temperature. The E_g values of all the samples were determined by plotting the logarithmic dependence of electrical conductivity *vs.* inverse of temperature ($1/T$), as shown in the inset of Fig. 5(b). Understanding this behavior is critical for optimizing thermoelectric performance. Upon Te-doping, the E_g value was initially increased due to increased defects, however, upon further increasing Te-contents, E_g was subsequently decreased due to higher intrinsic conductivity of Cu_2Te, as discussed earlier.[22,66]

The temperature dependent Seebeck coefficient (S) of all the samples showed positive values which confirms holes are the majority charge carriers, as shown in Fig. 5(c). At room temperature, the Seebeck coefficient of pure $Cu_{2-x}Se$ thin film is 28.35 μV K^{-1} and varies very little across the temperature range. For the Te-doped thin film with 5% Te, the Seebeck coefficient at room temperature is 30 μV K^{-1}, which is slightly higher than that of the pure sample. The highest Seebeck value of 64 μV K^{-1} at 400 K has been observed for Te-5%, which is about 100% larger than that of the pure sample at the same temperature. However, upon further increase in Te concentration results in the formation of Cu_2Te nanoclusters, which provide additional pathways for charge carriers. As stated above, Cu_2Te exhibits higher intrinsic electrical conductivity and a lower Seebeck coefficient compared to $Cu_{2-x}Se$.[67] The embedded Cu_2Te nanoclusters dominate carrier transport, resulting in a reduction of the Seebeck coefficient for all the samples having Te contents larger than 5%, which suggests that Te-5% is the optimal composition for maintaining a balance between electrical conductivity and the Seebeck coefficient. The striking increase in the Seebeck coefficient for the Te-5% sample at 400 K is attributed to the phase transition of α-Cu_2Se to β-Cu_2Se occurring at this temperature. This transition

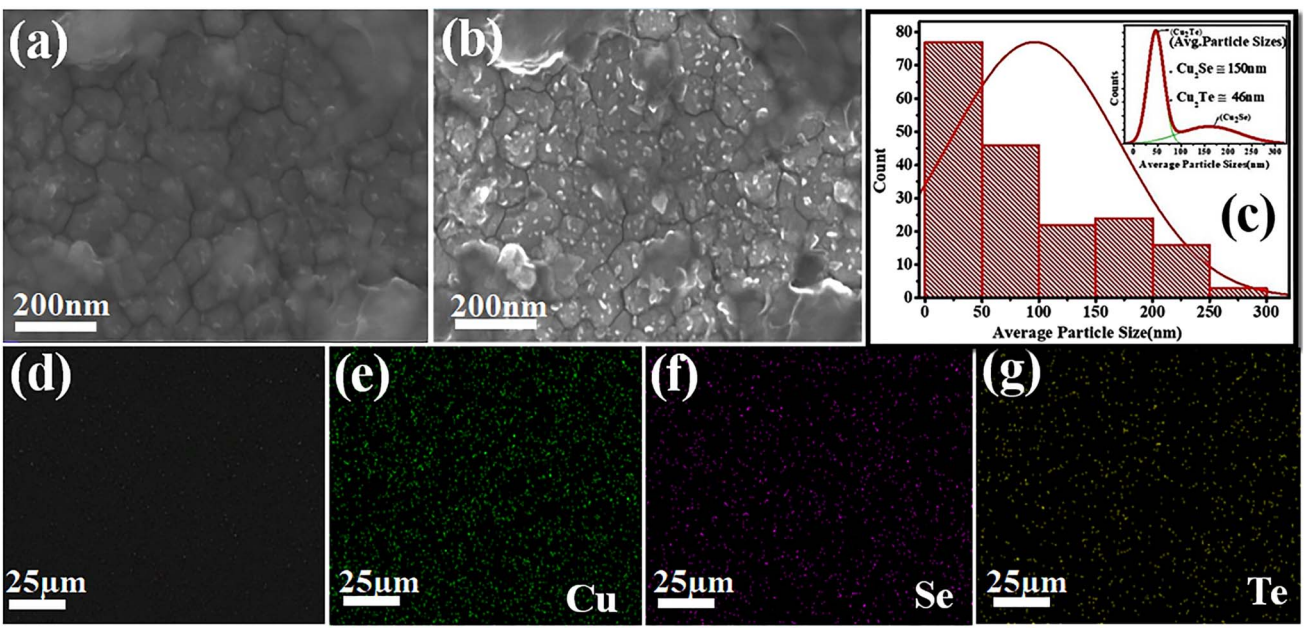

Fig. 4 Scanning electron microscopic (SEM) images of Te-20% doped thin film using (a) secondary electron, (b) in-lenz detector, (c) particle size, (d) SEM image used for elemental mapping of (e) Cu, (f) Se and (g) Te.

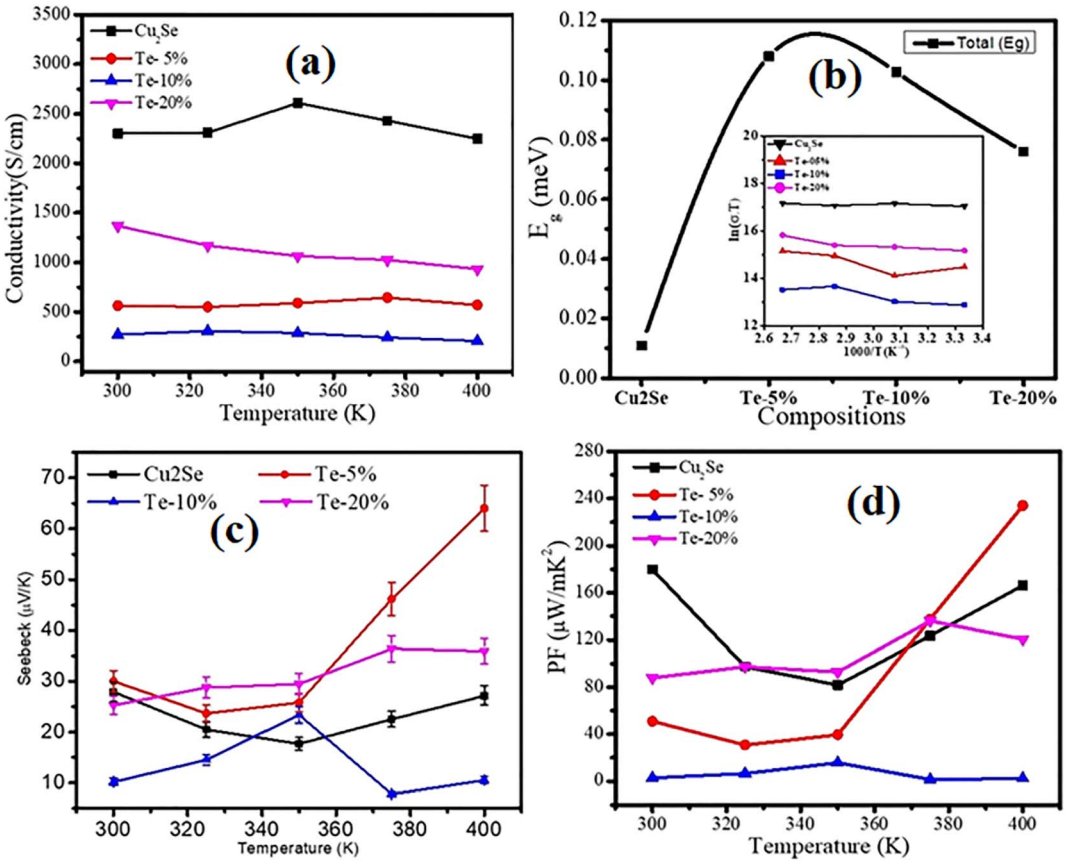

Fig. 5 Thermoelectric properties of Cu_2Se and Te-doped (5%, 10% and 20%) Cu_2Se thin films as a function of temperature: (a) electrical conductivity, (b) activation energy (E_g) for different compositions with an inset showing ln(σT) *vs.* 1000/T, (c) Seebeck coefficient, and (d) power factor (PF).

enhances carrier dynamics, amplifying the Seebeck effect.[68] Our highest Seebeck coefficient of 64 μV K^{-1}. In contrast, a study on polyaniline-Sb_2Te_3, Bi_2Te_3 thin films achieved a maximum Seebeck coefficient of approximately 30 μV K^{-1}.[69] This indicates that our film's Seebeck coefficient is over twice as high. The power factor (PF), derived from the Seebeck coefficient (S) and electrical conductivity (σ) is a critical parameter for evaluating thermoelectric performance. Fig. 5(d) shows the temperature dependent PF values of all the series. At 300 K, the (PF) of pure thin film is 97 μW mK^{-2} reaching its highest value of 166 μW mK^{-2} at 400 K. In the Te-doped series, (PF) value of Te-5% is 30 μW mK^{-2}, rising to a maximum of 234 μW mK^{-2} at 400 K, which is larger than that of the pure thin film. This significant improvement highlights the role of the Seebeck coefficient in optimizing PF. The highest PF of 234.0 μW m^{-1} K^{-2}, is lower than that of the α-Cu_2Se thin film's reported value.[70] Further increasing film's thickness (beyond 100 nm) or tuning annealing conditions could higher (PF), but we improve the power

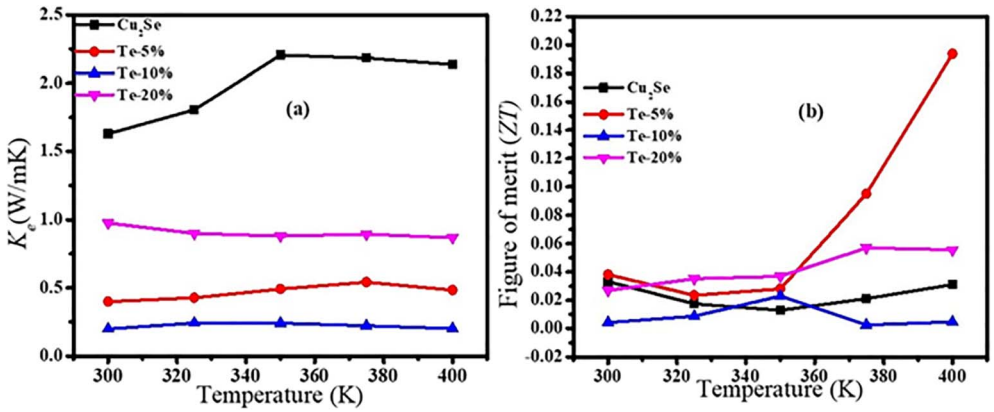

Fig. 6 Temperature dependence of (a) electronic thermal conductivity (K_e), (b) over-estimated figure of merit (ZT).

factor and Seebeck coefficient as compared to pure Cu_2Se thin films.

The experimental determination of total thermal conductivity (K_t) of thin films is challenging,[33] especially the lattice thermal conductivity (K_l). However, the electronic thermal conductivity (K_e) can be determined using the Wiedemann–Franz law: $K_e = L_o\sigma T$, where L_o is the Lorentz constant, (σ) is electrical conductivity, and T is the absolute temperature. For metallic and degenerate materials, $L_o \sim 2.44 \times 10^{-8}$ W Ω K^{-2} is the constant value.[71] However, the true Lorentz number values are calculated using single parabolic band coupled with acoustic phonon scattering.[67,71,72] The combined effect of nanoclusters, along with other defects, reduced K_e, as shown in Fig. 6(a), which results in an increased value for figure of merit (ZT) of the doped samples, as shown in Fig. 6(b). The ZT values were estimated by merely relying only on K_e while ignoring K_l due to the complexity and unavailability of methods to measure K_t of the thin film samples.[22] Thus, the estimated ZT is slightly overestimated, but it suggests a roadmap for the importance of thin films in the field of thermoelectric device miniaturization.

Conclusions

This work demonstrates that Te-doped Cu_2Se multiphase nanocomposite thin films exhibit substantial improvements in thermoelectric transport properties, exceeding pristine Cu_2Se thin films. The incorporation of Te promotes the formation of secondary phases, such as Cu_2Te nanoclusters and Te–Se solid solutions. Initially, Te-doping results in a decrease in electrical conductivity due to enormous carrier scattering against defects, but further increase in Te-doping enhances thermoelectric power factor through the synergy of optimized electrical conductivity and Seebeck coefficient. This composition, characterized by reduced electronic thermal conductivity and an enhanced power factor, attains a ZT of 0.2, reinforcing its applicability in thermoelectric systems. This study opens up new avenues for the incorporation of thin films into miniaturization of thermoelectric devices.

Data availability

Data will be provided upon request.

Conflicts of interest

All the authors declare that there is no conflict of interest.

Acknowledgements

All the authors are thankful to the Higher Education Commission (HEC) of Pakistan for financial support through the 8096/NRPU/R&D/HEC/2017 project.

References

1 E. Vieira, A. L. Pires, J. P. Silva, V. H. Magalhães, J. Grilo, F. Brito, M. Silva, A. Pereira and L. Goncalves, High-performance μ-thermoelectric device based on Bi2Te3/Sb2Te3 p–n junctions, *ACS Appl. Mater. Interfaces*, 2019, **11**(42), 38946–38954.
2 K. Biswas, J. He, I. D. Blum, C.-I. Wu, T. P. Hogan, D. N. Seidman, V. P. Dravid and M. G. Kanatzidis, High-performance bulk thermoelectrics with all-scale hierarchical architectures, *Nature*, 2012, **489**(7416), 414–418.
3 B. Sales, D. Mandrus, B. Chakoumakos, V. Keppens and J. Thompson, Filled skutterudite antimonides: Electron crystals and phonon glasses, *Phys. Rev. B:Condens. Matter Mater. Phys.*, 1997, **56**(23), 15081.
4 G. Ren, J. Lan, C. Zeng, Y. Liu, B. Zhan, S. Butt, Y.-H. Lin and C.-W. Nan, High Performance Oxides-Based Thermoelectric Materials, *JOM*, 2015, **67**(1), 211–221, DOI: **10.1007/s11837-014-1218-2**.
5 H. Han, L. Zhao, X. Wu, B. Zuo, S. Bian, T. Li, X. Liu, Y. Jiang, C. Chen, J. Bi, *et al.*, Advancements in thermoelectric materials: optimization strategies for enhancing energy conversion, *J. Mater. Chem. A*, 2024, **12**(36), 24041–24083, DOI: **10.1039/D4TA03666B**.
6 S. Butt, W. Xu, W. Q. He, Q. Tan, G. K. Ren, Y. Lin and C.-W. Nan, Enhancement of thermoelectric performance in Cd-doped Ca 3 Co 4 O 9 *via* spin entropy, defect chemistry and phonon scattering, *J. Mater. Chem. A*, 2014, **2**(45), 19479–19487.
7 S. Butt, Y.-C. Liu, J.-L. Lan, K. Shehzad, B. Zhan, Y. Lin and C.-W. Nan, High-temperature thermoelectric properties of La and Fe co-doped Ca–Co–O misfit-layered cobaltites consolidated by spark plasma sintering, *J. Alloys Compd.*, 2014, **588**, 277–283.
8 B. Zhan, S. Butt, Y. Liu, J.-L. Lan, C.-W. Nan and Y.-H. Lin, High-temperature thermoelectric behaviors of Sn-doped n-type Bi2O2Se ceramics, *J. Electroceram.*, 2015, **34**(2), 175–179, DOI: **10.1007/s10832-014-9969-2**.
9 Y.-c. Liu, Y.-h. Zheng, B. Zhan, K. Chen, S. Butt, B. Zhang and Y.-h. Lin, Influence of Ag doping on thermoelectric properties of BiCuSeO, *J. Eur. Ceram. Soc.*, 2015, **35**(2), 845–849, DOI: **10.1016/j.jeurceramsoc.2014.09.015**.
10 C. Zeng, S. Butt, Y.-H. Lin, M. Li and C.-W. Nan, Enhanced Thermoelectric Performance of SmBaCuFeO5+δ/Ag Composite Ceramics, *J. Am. Ceram. Soc.*, 2016, **99**(4), 1266–1270, DOI: **10.1111/jace.14062**.
11 W. Xu, S. Butt, Y. Zhu, J. Zhou, Y. Liu, M. Yu, A. Marcelli, J. Lan, Y.-H. Lin and C.-W. Nan, Nanoscale heterogeneity in thermoelectrics: the occurrence of phase separation in Fe-doped Ca3Co4O9, *Phys. Chem. Chem. Phys.*, 2016, **18**(21), 14580–14587, DOI: **10.1039/C6CP00819D**.
12 S. Butt, W. Xu, M. U. Farooq, G. K. Ren, F. Mohmed, Y. Lin and C. W. Nan, Enhancement of Thermoelectric Performance in Hierarchical Mesoscopic Oxide Composites of Ca3Co4O9and La0.8Sr0.2CoO3, *J. Am. Ceram. Soc.*, 2015, **98**(4), 1230.
13 C. Uher, Thermoelectric properties of Skutterudites, in *Thermoelectric Energy Conversion*, Elsevier, 2021, pp. 69–123.
14 J. Mi, T. Zhu, X. Zhao and J. Ma, Nanostructuring and thermoelectric properties of bulk skutterudite compound CoSb3, *J. Appl. Phys.*, 2007, **101**(5), 054314.

15 M. Oudah, K. M. Kleinke and H. Kleinke, Thermoelectric properties of the quaternary chalcogenides BaCu5. 9STe6 and BaCu5. 9SeTe6, *Inorg. Chem.*, 2015, **54**(3), 845–849.
16 M.-L. Liu, I.-W. Chen, F.-Q. Huang and L.-D. Chen, Improved thermoelectric properties of Cu-doped quaternary chalcogenides of Cu2CdSnSe4, *Adv. Mater.*, 2009, **21**(37), 3808–3812.
17 H. Liu, X. Yuan, P. Lu, X. Shi, F. Xu, Y. He, Y. Tang, S. Bai, W. Zhang, L. Chen, *et al.*, Ultrahigh Thermoelectric Performance by Electron and Phonon Critical Scattering in $Cu_2Se_{1-x}I_x$, *Adv. Mater.*, 2013, **25**(45), 6607.
18 H. Kim, S. Ballikaya, H. Chi, J. P. Ahn, K. Ahn, C. Uher and M. Kaviany, Ultralow Thermal Conductivity of Cu_2Se by Atomic Fluidity and Structure Distortion, *Acta Mater.*, 2015, **86**, 247.
19 S. Butt, M. U. Farooq, W. Mahmood, S. Salam, M. Sultan, M. A. Basit, J. Ma, Y. Lin and C.-W. Nan, One-step rapid synthesis of Cu_2Se with enhanced thermoelectric properties, *J. Alloys Compd.*, 2019, **786**, 557–564, DOI: **10.1016/j.jallcom.2019.01.359**.
20 M. U. Farooq, S. Butt, K. Gao, X. Sun, X. Pang, S. U. Khan, W. Xu, F. Mohmed, A. Mahmood and N. Mahmood, Enhanced thermoelectric efficiency of $Cu_{2-x}Se$–Cu_2S composite by incorporating Cu_2S nanoparticles, *Ceram. Int.*, 2016, **42**(7), 8395–8401, DOI: **10.1016/j.ceramint.2016.02.055**.
21 S. Butt, W. Xu, M. U. Farooq, G. K. Ren, Q. Zhang, Y. Zhu, S. U. Khan, L. Liu, M. Yu, F. Mohmed, *et al.*, Enhanced Thermoelectricity in High-Temperature β-Phase Copper(I) Selenides Embedded with Cu_2Te Nanoclusters, *ACS Appl. Mater. Interfaces*, 2016, **8**(24), 15196–15204, DOI: **10.1021/acsami.6b02086**.
22 Sumayya, S. Butt, M. U. Farooq, M. A. Basit, U. Ali and M. A. Akram, Improved thermoelectric power factor of multilayered poly(3,4-ethylenedioxythiophene) polystyrene sulfonate and Cu_2Se thin films, *Thin Solid Films*, 2023, **784**, 140090, DOI: **10.1016/j.tsf.2023.140090**.
23 M. Irfan, S. Butt, Sumayya, M. W. Akram, M. Saadullah, M. A. Basit, J. Ahmad, M. Yasir and H. Ozair, Unlocking the effect of film thickness on the thermoelectric properties of thermally evaporated $Cu_{2-x}Se$ thin films, *RSC Adv.*, 2024, **14**(51), 37688–37695, DOI: **10.1039/D4RA06908K**.
24 S. K. Kihoi, T.-Y. Yang and H. S. Lee, Recent Progress in SnTe: An Eco-Friendly and High-Performance Chalcogenide Thermoelectric Material, *Small*, 2409315, DOI: **10.1002/smll.202409315**.
25 N.-H. Li, Q. Zhang, X.-L. Shi, J. Jiang and Z.-G. Chen, Silver Copper Chalcogenide Thermoelectrics: Advance, Controversy, and Perspective, *Adv. Mater.*, 2024, **36**(37), 2313146, DOI: **10.1002/adma.202313146**.
26 C. Gayner, R. Sharma, I. Mallik, M. K. Das and K. K. Kar, Exploring the doping effects of copper on thermoelectric properties of lead selenide, *J. Phys. D: Appl. Phys.*, 2016, **49**(28), 285104.
27 B. Gahtori, S. Bathula, K. Tyagi, M. Jayasimhadri, A. Srivastava, S. Singh, R. Budhani and A. Dhar, Giant enhancement in thermoelectric performance of copper selenide by incorporation of different nanoscale dimensional defect features, *Nano Energy*, 2015, **13**, 36–46.
28 S. Butt, Y. Ren, M. U. Farooq, B. Zhan, R. U. R. Sagar, Y. Lin and C. W. Nan, Enhanced Thermoelectric Performance of Heavy-Metals (M: Ba, Pb) Doped Misfit-Layered Ceramics: (Ca2–xMxCoO3)0.62 (CoO2), *Energy Convers. Manage.*, 2014, **83**, 35.
29 Z. Afzal, S. Butt, M. Rizwan, S. U. Rehman, S. Sajjad, Z. Usman and G. M. Murtaza, Density Functional Theory (DFT) perspectives of thermoelectric transportation in Sr-doped LaCoO3, *Next Materials*, 2025, **7**, 100383, DOI: **10.1016/j.nxmate.2024.100383**.
30 F. F. Jaldurgam, Z. Ahmad, F. Touati, A. Al Ashraf, A. Shakoor, J. Bhadra, N. J. Al-Thani and T. Altahtamouni, Enhancement of thermoelectric properties of low-toxic and earth-abundant copper selenide thermoelectric material by microwave annealing, *J. Alloys Compd.*, 2022, **904**, 164131.
31 Y. Zhang, Z. P. Qiao and X. M. Chen, Microwave-Assisted Elemental Direct Reaction Route to Nanocrystalline Copper Chalcogenides CuSe and Cu_2Te, *J. Mater. Chem.*, 2002, **12**(9), 2747.
32 I. Chowdhury, R. Prasher, K. Lofgreen, G. Chrysler, S. Narasimhan, R. Mahajan, D. Koester, R. Alley and R. Venkatasubramanian, On-Chip Cooling by Superlattice-Based Thin-Film Thermoelectrics, *Nat. Nanotechnol.*, 2009, **4**(4), 235.
33 A. Minnich, M. S. Dresselhaus, Z. Ren and G. Chen, Bulk nanostructured thermoelectric materials: current research and future prospects, *Energy Environ. Sci.*, 2009, **2**(5), 466–479.
34 B. Yu, W. Liu, S. Chen, H. Wang, G. Chen and Z. Ren, Thermoelectric Properties of Copper Selenide with Ordered Selenium Layer and Disordered Copper Layer, *Nano Energy*, 2012, **1**(3), 472.
35 J. Yu, H. Hu, H.-L. Zhuang, H. Li and J.-F. Li, Stabilization of Superionic Copper Selenide Based Thermoelectric Materials, *Acc. Mater. Res.*, 2024, 1428–1439.
36 L.-D. Zhao, S.-H. Lo, Y. Zhang, H. Sun, G. Tan, C. Uher, C. Wolverton, V. P. Dravid and M. G. Kanatzidis, Ultralow thermal conductivity and high thermoelectric figure of merit in SnSe crystals, *nature*, 2014, **508**(7496), 373–377.
37 X. Chen, J. Yang, T. Wu, L. Li, W. Luo, W. Jiang and L. Wang, Nanostructured binary copper chalcogenides: synthesis strategies and common applications, *Nanoscale*, 2018, **10**(32), 15130–15163.
38 X.-X. Xiao, W.-J. Xie, X.-F. Tang and Q.-J. Zhang, Phase transition and high temperature thermoelectric properties of copper selenide $Cu_{2-x}Se$ ($0 \leq x \leq 0.25$), *Chin. Phys. B*, 2011, **20**(8), 087201.
39 S. Butt, W. Xu, M. U. Farooq, G. K. Ren, Q. Zhang, Y. Zhu, S. U. Khan, L. Liu, M. Yu and F. Mohmed, Enhanced thermoelectricity in high-temperature β-phase copper (I) selenides embedded with Cu_2Te nanoclusters, *ACS Appl. Mater. Interfaces*, 2016, **8**(24), 15196–15204.
40 L. Yang, Z.-G. Chen, G. Han, M. Hong and J. Zou, Impacts of Cu deficiency on the thermoelectric properties of $Cu_{2-x}Se$ nanoplates, *Acta Mater.*, 2016, **113**, 140–146.

41 C. Rudradawong, S. Khammuang, K. Kotmool, T. Bovornratanaraks, P. Limsuwan, N. Somdock, R. Sakdanuphab and A. Sakulkalavek, Enhanced thermoelectric properties of Cu_2Se *via* Sb doping: An experimental and computational study, *J. Eur. Ceram. Soc.*, 2023, **43**(2), 401–406.

42 P. Banerjee, *Exploring Condensed Phases in Engineered Semiconducting Nanocrystals*, University of Illinois at Urbana-Champaign, 2018.

43 B. J. Stanbery, Copper indium selenides and related materials for photovoltaic devices, *Crit. Rev. Solid State Mater. Sci.*, 2002, **27**(2), 73–117.

44 H. Liu, X. Shi, F. Xu, L. Zhang, W. Zhang, L. Chen, Q. Li, C. Uher, T. Day and G. J. Snyder, Copper ion liquid-like thermoelectrics, *Nat. Mater.*, 2012, **11**(5), 422–425, DOI: **10.1038/nmat3273**.

45 P. Lu, H. Liu, X. Yuan, F. Xu, X. Shi, K. Zhao, W. Qiu, W. Zhang and L. Chen, Multiformity and fluctuation of Cu ordering in Cu 2 Se thermoelectric materials, *J. Mater. Chem. A*, 2015, **3**(13), 6901–6908.

46 L.-l. Zhao, X.-l. Wang, J.-y. Wang, Z.-x. Cheng, S.-x. Dou, J. Wang and L.-q. Liu, Superior intrinsic thermoelectric performance with zT of 1.8 in single-crystal and melt-quenched highly dense $Cu_{2-x}Se$ bulks, *Sci. Rep.*, 2015, **5**(1), 7671.

47 H. Liu, X. Shi, M. Kirkham, H. Wang, Q. Li, C. Uher, W. Zhang and L. Chen, Structure-transformation-induced abnormal thermoelectric properties in semiconductor copper selenide, *Mater. Lett.*, 2013, **93**, 121–124.

48 T. W. Day, K. S. Weldert, W. G. Zeier, B.-R. Chen, S. L. Moffitt, U. Weis, K. P. Jochum, M. Panthöfer, M. J. Bedzyk and G. J. Snyder, Influence of Compensating Defect Formation on the Doping Efficiency and Thermoelectric Properties of $Cu_{2-y}Se_{1-x}Br_x$, *Chem. Mater.*, 2015, **27**(20), 7018–7027.

49 F. Rong, Y. Bai, T. Chen and W. Zheng, Chemical synthesis of Cu_2Se nanoparticles at room temperature, *Mater. Res. Bull.*, 2012, **47**(1), 92–95, DOI: **10.1016/j.materresbull.2011.09.026**.

50 S. Ballikaya, H. Chi, J. R. Salvador and C. Uher, Thermoelectric properties of Ag-doped Cu_2Se and Cu_2Te, *J. Mater. Chem. A*, 2013, **1**(40), 12478–12484, DOI: **10.1039/C3TA12508D**.

51 H. Liu, X. Yuan, P. Lu, X. Shi, F. Xu, Y. He, Y. Tang, S. Bai, W. Zhang and L. Chen, Ultrahigh Thermoelectric Performance by Electron and Phonon Critical Scattering in $Cu_2Se_{1-x}I_x$, *Adv. Mater.*, 2013, 6607–6612.

52 L. Yang, Z.-G. Chen, G. Han, M. Hong, L. Huang and J. Zou, Te-Doped Cu 2 Se nanoplates with a high average thermoelectric figure of merit, *J. Mater. Chem. A*, 2016, **4**(23), 9213–9219.

53 B. Yu, W. Liu, S. Chen, H. Wang, H. Wang, G. Chen and Z. Ren, Thermoelectric properties of copper selenide with ordered selenium layer and disordered copper layer, *Nano Energy*, 2012, **1**(3), 472–478, DOI: **10.1016/j.nanoen.2012.02.010**.

54 C. Du, M. Cao, G. Li, Y. Hu, Y. Zhang, L. Liang, Z. Liu and G. Chen, Toward precision recognition of complex hand motions: wearable thermoelectrics by synergistic 2D nanostructure confinement and controlled reduction, *Adv. Funct. Mater.*, 2022, **32**(36), 2206083.

55 C. Chen, Z. Liu, L. Guo, B. Huo, Q. Sun, L. Liang, C. Du and G. Chen, High Spatiotemporal Resolution Biomimetic Thermoreceptors Realizing by Jointless p-n Integration Thermoelectric Composites, *Adv. Funct. Mater.*, 2024, **34**(49), 2411490.

56 L. Tang, K. Ruan, X. Liu, Y. Tang, Y. Zhang and J. Gu, Flexible and robust functionalized boron nitride/poly (p-phenylene benzobisoxazole) nanocomposite paper with high thermal conductivity and outstanding electrical insulation, *Nano-Micro Lett.*, 2024, **16**(1), 38.

57 X. Si, Q. Zhang, X. Guo, J. Yang, T. Zhao and Y. Zhang, Bioinspired Chestnut Burr-like Polyaniline: Achieving Superhydrophobicity and Excellent Microwave Transparency through Controlled Polymerization, *ACS Appl. Mater. Interfaces*, 2025, 9867–9878.

58 Q. Meng, H. Song, Y. Du, Y. Ding and K. Cai, Facile preparation of poly(3,4-ethylenedioxythiophene): poly(styrenesulfonate)/Ag2Te nanorod composite films for flexible thermoelectric generator, *J. Materiomics*, 2021, **7**(2), 302–309, DOI: **10.1016/j.jmat.2020.10.011**.

59 J. D. Forster, J. J. Lynch, N. E. Coates, J. Liu, H. Jang, E. Zaia, M. P. Gordon, M. Szybowski, A. Sahu, D. G. Cahill, *et al.*, Solution-Processed Cu_2Se Nanocrystal Films with Bulk-Like Thermoelectric Performance, *Sci. Rep.*, 2017, **7**(1), 2765, DOI: **10.1038/s41598-017-02944-1**.

60 Z. Wu, J. Wu, Y. Li and G. Li, Effect of Cu content on electrical properties of evaporated Cu-Se thermoelectric films, *Ceram. Int.*, 2020, **46**(13), 21617–21622.

61 J. A. Perez-Taborda, L. Vera, O. Caballero-Calero, E. O. Lopez, J. J. Romero, D. G. Stroppa, F. Briones and M. Martin-Gonzalez, Pulsed hybrid reactive magnetron sputtering for high zT Cu_2Se thermoelectric films, *Adv. Mater. Technol.*, 2017, **2**(7), 1700012.

62 Z. Lin, C. Hollar, J. S. Kang, A. Yin, Y. Wang, H. Y. Shiu, Y. Huang, Y. Hu, Y. Zhang and X. Duan, A solution processable high-performance thermoelectric copper selenide thin film, *Adv. Mater.*, 2017, **29**(21), 1606662.

63 M. R. Scimeca, F. Yang, E. Zaia, N. Chen, P. Zhao, M. P. Gordon, J. D. Forster, Y.-S. Liu, J. Guo, J. J. Urban, *et al.*, Rapid Stoichiometry Control in Cu_2Se Thin Films for Room-Temperature Power Factor Improvement, *ACS Appl. Energy Mater.*, 2019, **2**(2), 1517–1525, DOI: **10.1021/acsaem.8b02118**.

64 M. R. Scimeca, F. Yang, E. Zaia, N. Chen, P. Zhao, M. P. Gordon, J. D. Forster, Y.-S. Liu, J. Guo and J. J. Urban, Rapid stoichiometry control in Cu_2Se thin films for room-temperature power factor improvement, *ACS Appl. Energy Mater.*, 2019, **2**(2), 1517–1525.

65 S. Butt, N. A. Shah, A. Nazir, Z. Ali and A. Maqsood, Influence of film thickness and In-doping on physical properties of CdS thin films, *J. Alloys Compd.*, 2014, **587**, 582–587, DOI: **10.1016/j.jallcom.2013.10.221**.

66 N. Naeem, S. Butt, Sumayya, Z. Afzal, M. Waseem Akram, M. Irfan, M. Atiq Ur Rehman, A. H. Baluch, G. u. Rehman

and M. U. Farooq, Facile development of carbon nanotube (CNT)-based flexible thermoelectric materials for energy-harvesting applications, *RSC Adv.*, 2025, **15**(1), 569–578, DOI: 10.1039/D4RA02914C.

67 S. Ballikaya, H. Chi, J. R. Salvador and C. Uher, Thermoelectric properties of Ag-doped Cu 2 Se and Cu 2 Te, *J. Mater. Chem. A*, 2013, **1**(40), 12478–12484.

68 G. Mahan, The Seebeck coefficient of superionic conductors, *J. Appl. Phys.*, 2015, **117**(4), 045101.

69 M. R. Roknabadi, M. Mollaee and S. Garazhian, Fabrication and thermoelectric properties of nano Sb2Te3, Bi2Te3 thin films using PVD of synthesized nano powder, *J. Mater. Sci.: Mater. Electron.*, 2025, **36**(3), 1–10.

70 P. Fan, X.-l. Huang, T.-b. Chen, F. Li, Y.-x. Chen, B. Jabar, S. Chen, H.-l. Ma, G.-x. Liang and J.-t. Luo, α-Cu_2Se thermoelectric thin films prepared by copper sputtering into selenium precursor layers, *Chem. Eng. J.*, 2021, **410**, 128444.

71 M. U. Iqbal, Sumayya, S. Butt, M. U. Farooq, S. Hussain, S. Irfan, N. Ali, M. A. Basit, M. A. Akram, M. Yasir, *et al.*, Thermoelectric transportation in Cu-added Ca3Co4O9 ceramics consolidated by spark plasma sintering, *Phys. B*, 2023, **654**, 414738, DOI: 10.1016/j.physb.2023.414738.

72 L. Yang, J. Wei, Y. Qin, L. Wei, P. Song, M. Zhang, F. Yang and X. Wang, Thermoelectric properties of Cu_2Se nano-thin film by magnetron sputtering, *Materials*, 2021, **14**(8), 2075.